Homogeneous reporter system enables quantitative functional assessment of multiple transcription factors

Sergei Romanov[1], Alexander Medvedev[1], Maria Gambarian[1], Natalia Poltoratskaya[1], Matt Moeser[1], Liubov Medvedeva[1], Mikhail Gambarian[2], Luda Diatchenko[3] & Sergei Makarov[1]

We developed a high-content reporter system that allows quantitative assessment of activities of multiple transcription factors (TFs) in a eukaryotic cell. The system comprises a library of reporter constructs that are evaluated according to their transcription rates. All reporters produce essentially identical messages that are subjected to 'processing', which generates a spectrum of distinguishable fragments that are analyzed quantitatively. The homogeneity of the reporter library afforded inherently uniform detection conditions for all reporters and provided repeatability, accuracy and robustness of assessment. We showed that this technology can be used to identify pathways transmitting cell responses to inducers, and that the profile of TF activities generated using this system represents a stable and sustained cell signature that clearly distinguishes different cell types and pathological conditions. This technology provides a framework for functional characterization of signal transduction networks through profiling activities of multiple TFs.

The cellular gene regulatory network comprises many interacting signal transduction pathways. At the apexes of many pathways are TFs, which are DNA-binding proteins that recognize specific sequences within regulatory regions of target genes and thereby modulate their transcription. It has been estimated that mammalian genomes encode about 2,000 of TFs that may be divided into 150–400 of families according to similarities of their DNA-binding motifs[1–3]. By surveying activities of the multiple TFs one should be able to obtain a snapshot that comprehensively characterizes functional state of a gene regulatory network. However, this approach requires adequate tools for high-content TF analysis.

Transcriptional activity of a TF is defined by its ability to activate or suppress transcription. TF activity is regulated by various post-translational modifications of pre-existing TFs, and thus the protein content does not reflect the TF's functional status. Many TFs are regulated thru modulation of their DNA-binding properties, and thus DNA-binding assays are frequently used to measure TF activation, including multiplexing assays that can evaluate several TFs at a time[4,5]. But although DNA binding is a prerequisite for transcription, a TF's activity can be modulated independently from DNA binding, for example, through many TF modifications that alter TF interactions with corepressors and coactivators. For example, many nuclear receptors are constitutively bound to their cognate DNA sequences, but their transcriptional activities are specifically regulated by ligands[6]. Therefore, DNA binding is only a surrogate indicator of TF activity.

A gold standard for functional TF assessment has been a reporter gene assay that makes use of a reporter gene construct wherein a TF-responsive promoter controls expression of a gene encoding an easily assayable reporter protein[7]. However, owing to a limited repertoire of reporter proteins, these assays are useful for assessments of very few TFs at a time. Another problem is that reporter proteins may be unpredictably affected by irrelevant post-transcriptional mechanisms[8].

These limitations can be obviated by using multiple reporter constructs with different reporter sequences that are evaluated according to their transcription rates, for example, by hybridizing the reporter transcripts to a detection array[9]. However, the innate heterogeneity of reporter sequences is a major problem because distinct reporter sequences are transcribed with different efficacies, their transcripts have different secondary structures and stabilities[10], and their half-lives may be differentially affected by various extracellular stimuli[11]. These problems may have detrimental effects on the linearity, accuracy and reproducibility of assay.

Here we describe a high-capacity reporter system that makes use of highly similar reporter constructs that generate nearly identical reporter transcripts. To distinguish these transcripts, we used a procedure referred to as 'processing', which produces distinct DNA fragments that are quantitatively evaluated by capillary electrophoresis. This detection approach virtually eliminated nonspecific detection background, and the similarity of the reporter constructs brought about an inherent uniformity of individual assessments, thus affording repeatability, accuracy and robustness of the

[1]Attagene Inc., P.O. Box 12054, Research Triangle Park, North Carolina 27709, USA. [2]MishaGam Software, 525 Riverside Ln., Cayce, South Carolina 29033, USA. [3]Center for Neurosensory Disorders, 2120 Old Dental Building, CB 7450, University of North Carolina at Chapel Hill, Chapel Hill, North Carolina 27599, USA. Correspondence should be addressed to S.M. (smak@attagene.com).

RECEIVED 1 DECEMBER 2007; ACCEPTED 28 JANUARY 2008; PUBLISHED ONLINE 24 FEBRUARY 2008; DOI:10.1038/NMETH.1186

multiplexing detection. Furthermore, the TF activity profiles obtained with our technology represented robust and sustained cell signatures, and provided invaluable information about the state of a gene regulatory network.

RESULTS

Library of homogenous reporter transcription units

A core component of our system is a library of reporter constructs that we termed 'reporter transcription units' (RTUs). An RTU resembles a conventional reporter gene construct in that it has a TF-responsive promoter linked to a downstream reporter sequence. RTU transcripts are not translated into proteins; instead, we evaluated RTU activities by directly assessing reporter-transcript abundance.

A principal and distinct feature of our approach is that all RTUs have essentially identical reporter sequences (**Fig. 1a** and **Supplementary Fig. 1** online). To distinguish individual reporter transcripts, reporter sequences are tagged with 'processing tags' that represent an endonuclease recognition site (for example, *Hpa*I) that defines a unique cleavage position for each reporter cDNA (**Fig. 1a**

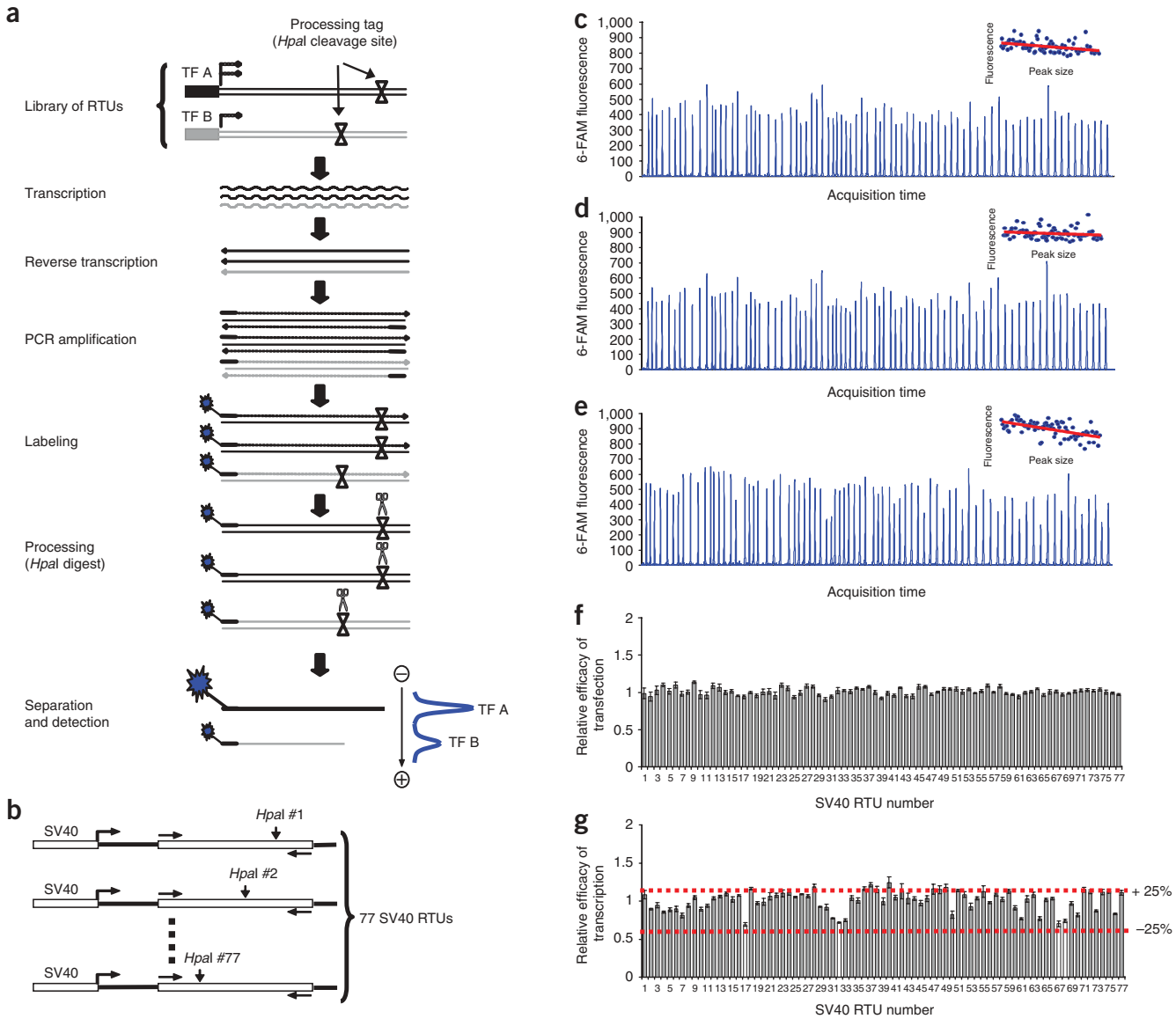

Figure 1 | Reporter system for functional assessment of multiple TFs. (**a**) Outline of the method. The two shown RTUs respond to TFs A and B. After transfection of RTUs into cells of interest, total RNA is isolated, reverse-transcribed, amplified, fluorescently labeled, processed, and the resulting fragments are quantified by capillary electrophoresis. (**b**) The auxiliary reporter library is a mix of 77 individual SV40 RTU plasmids at approximately equimolar ratio. (**c**,**d**) Electrophoregrams representing profiles of relative DNA concentrations of RTUs in the library (**c**) and in DNA isolated from transfected HepG2 cells (**d**) obtained using the modified MRTU detection protocol, that is, omitting the reverse transcription and DNAse treatment. (**e**) Electrophoregram representing profile of relative concentrations of RTU transcripts obtained by analyzing total RNA from transfected cells according to the original MRTU detection protocol. Insets illustrate that fluorescence intensities of the peaks reversely correlate with their sizes. To account for this artifact, peak intensities were corrected by using the approximating trend line. (**f**,**g**) Relative transfection (**f**) and transcription (**g**) efficacies of the individual SV40 RTUs calculated from the primary electrophoregrams (**c**–**e**). Shown are mean values of three independent experiments performed in parallel; error bars, s.d.

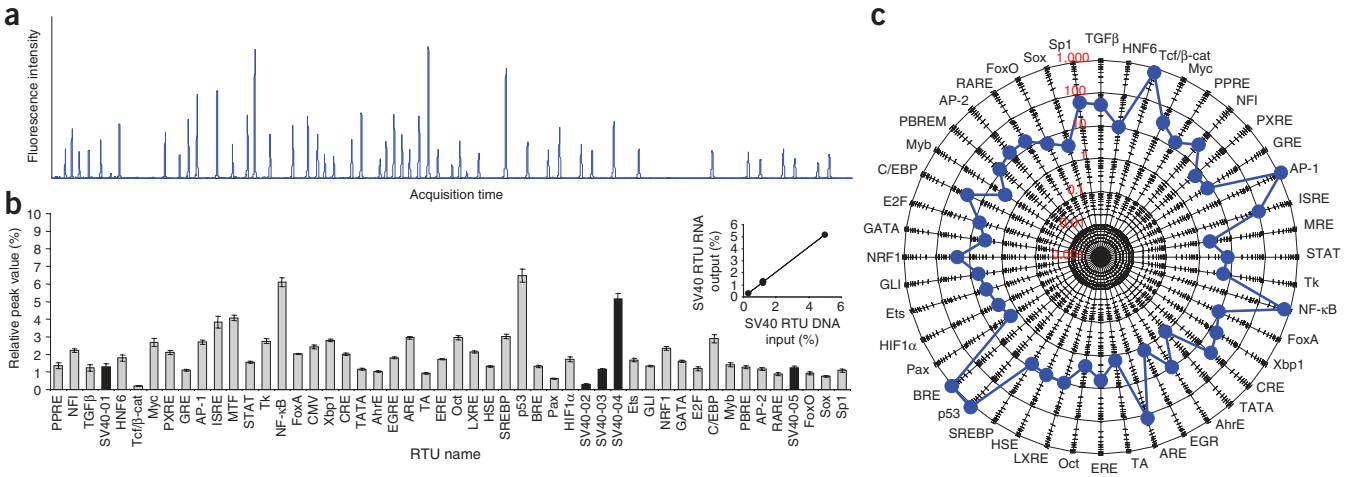

Figure 2 | TF activity profile in HepG2 cells transiently transfected with the RTU library. (**a**) Representative primary readout capillary electrophoregram for individual RTUs. (**b**) Standardized MRTU assay readout obtained by normalizing the signals of individual peaks to the sum of signals of all peaks. Means of data (± s.d.) obtained in 6 parallel experiments. Inset illustrates linearity ($R^2 = 0.9992$) of signals generated by five calibrating SV40 RTUs (black bars) that were present in the reporter library at defined concentrations. (**c**) The basal TF activity profile in HepG2 cells. Standardized capillary electrophoresis peak values (**b**) were normalized to the DNA inputs of the corresponding RTUs and divided by the normalized value of TATA RTU. Signals of calibrating SV40 RTUs are not shown. Each point represents a mean of six independent experiments performed in parallel. Note that radial graph has logarithmically scaled axes.

and **Supplementary Fig. 1**). For multiplexing, a library of multiple RTUs (MRTU library) is introduced into cells of interest; subsequently total RNA is isolated and reverse transcribed into cDNA. The reporter cDNAs are amplified using a pair of primers that is common for all RTUs, labeled with a fluorescent label, and processed by the *Hpa*I digest. The digest produces a spectrum of DNA fragments of different lengths that are resolved by capillary electrophoresis and detected as separate fluorescent peaks (**Fig. 1a**).

We expected the reporter transcripts to have equal transcription efficacies resulting in highly uniform detection conditions for all the RTUs. To test this assumption, we constructed an auxiliary SV40-MRTU library wherein all RTUs had an identical SV40 promoter and reporter sequences that differed only by the *Hpa*I tag position (**Fig. 1b**). We introduced this auxiliary library into HepG2 cells and determined the relative concentrations of individual reporter transcripts using the MRTU detection protocol. We normalized these data to the profile of relative DNA concentrations of the individual RTU plasmids taken up by the cells (**Fig. 1c–e**). The profile of relative concentrations of individual SV40 RTU plasmids in cells (**Fig. 1d**) was identical to that in the transfected plasmid library (**Fig. 1c**), indicating that representation of the individual RTUs was not altered after transfection (**Fig. 1f**). The vast majority of the Hpa1-tagged SV40 RTUs had very similar transcription efficiencies (**Fig. 1g**). Notably, we observed this uniformity of detection of the individual RTUs in a diverse set of human and mouse cell types, and it was not affected by various extracellular stimuli (**Supplementary Fig. 2** online). Thus, in most cases, introduction of the *Hpa*I processing tag did not substantially affect properties of reporter sequences and their transcripts.

We then used the *Hpa*I-tagged reporter sequences from the SV40 RTUs to construct TF-inducible RTUs whose promoters were typically made of single or multiple copies of TF DNA-binding sequences (for example, NF-κB, AP-1, c-Myc, HIF-1α and others; see **Supplementary Tables 1** and **2** online for a complete list of TF-inducible promoters and their binding sequences). We also used several stimulus-specific promoters to construct RTUs that were rendered specifically responsive to particular extracellular stimuli (for example, to: bone morphogenic proteins, BRE RTU; transforming growth factor beta, TGFβ RTU; and xenobiotics, PXRE RTU) rather than to a particular TF. Along with the inducible elements, each RTU promoter had a common, minimal, TATA-like sequence to facilitate recruitment of basal transcriptional machinery (**Supplementary Fig. 1**). In the vast majority of experiments, we introduced RTUs into cells as circular rather than linearized plasmids because the former one afforded substantially better efficacy of transfection. To minimize contribution of transcriptional readthrough from the vector backbone, all RTUs contained transcription termination signal (comprising synthetic polyadenylation site[12] and transcription pause site from human α2 globin gene[13]) that were positioned upstream of the TF-inducible promoters (**Supplementary Fig. 1**). Having validated the inducibility of individual RTUs' promoters in separate experiments (**Supplementary Fig. 3** and **Supplementary Table 3** online), we assembled the RTUs into a prototypical MRTU library comprising 43 TF- or stimulus-inducible RTUs, the TATA RTU (which had the common minimal TATA promoter), and several auxiliary SV40 RTUs that we included for calibration purposes.

Analyzing basal TF activity profile of cell

To obtain the basal TF activity profile of a cell, we transfected the MRTU library into cells of interest (in the example shown in **Fig. 2**, HepG2 cell line), and processed total cellular RNA according to the MRTU detection protocol. The primary readout of the assay is the electrophoregram (**Fig. 2a**) wherein the individual peaks reflect activities of corresponding RTUs. The standardized capillary electrophoresis peak's values (in percent of the sum of all peaks) represent the relative concentrations of the individual RTU transcripts (**Fig. 2b**). To account for variations in RTU plasmid

concentrations, we normalized the standardized capillary electrophoresis peak values based on the corresponding DNA concentrations, thus generating the profile of specific RTU activities that we consider as *bona fide* TF activity profile. We presented the specific RTU activities as fold-induction values of the individual RTUs versus the TATA RTU, which contains only the TATA-like sequence that is common to all RTUs in the library and thus accounts for the nonspecific basal transcription (**Fig. 2c**). In example shown in **Figure 2c**, the fold induction values of PAX, MRE and EGR RTUs were close to 1.0, indicating that the *cis* elements of these promoters did not enhance the basal transcription and thus suggesting minimal activation of the corresponding TFs. In contrast, specific activities of AP-1, Tcf/β-cat, p53 and NF-κB RTUs exceeded that of the TATA RTU by 100–1,000 fold, indicating strong constitutive activation of these TFs.

MRTU assay validation

We evaluated repeatability, linearity and robustness of the MRTU assay. Having compared TF activity profiles for multiple replicates, we found that the standard deviation values of individual RTU activities were in the range of 1–14% of their mean values (**Fig. 2b**), with a median of 5%, which is comparable with the repeatability of

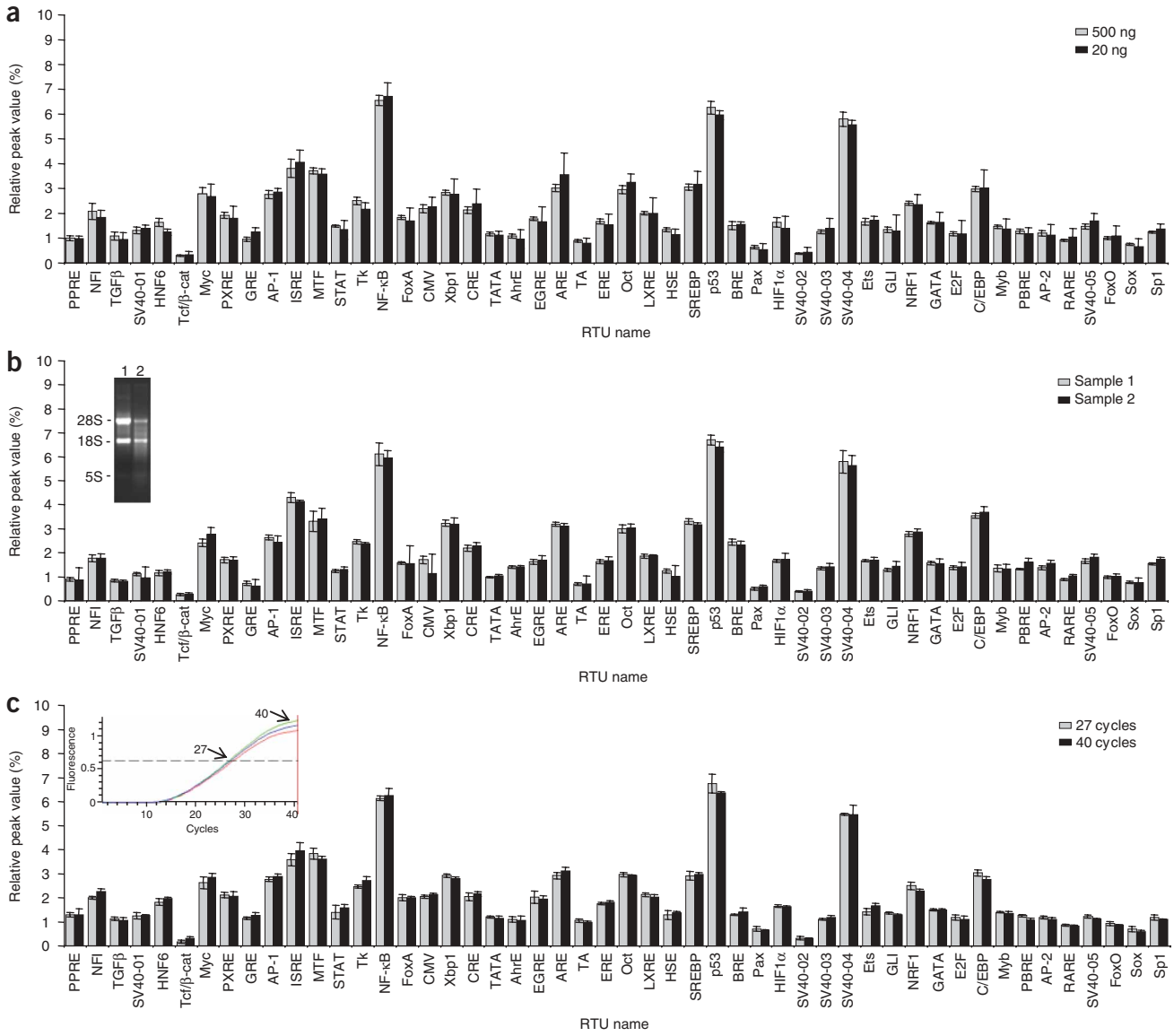

Figure 3 | Robustness of the MRTU assay. (**a**) MRTU assay in HepG2 cells transfected with 20 ng or with 500 ng of the MRTU library. The total amount of DNA in transfections was kept constant at 1 μg by adding an irrelevant carrier DNA. The relative activities of individual RTUs were calculated as described in **Figure 2b**. Shown are mean values ±s.d. of three independent experiments performed in parallel. (**b**) Two independent MRTU experiments in HepG2 cells produced RNA that had apparently different degradation (inset). Each RNA sample was analyzed in triplicate by using MRTU detection protocol, and data were calculated as described in **Figure 2b**. The bars represent mean values ±s.d. of the three assessments. (**c**) Aliquots of one RNA sample generated during MRTU assay in HepG2 cells were amplified by using variable numbers of PCR cycles. Each PCR condition was repeated in triplicate. The progress of amplification was monitored by quantitative real-time PCR performed in parallel (inset). The PCR products were collected after 27 cycles (exponential phase of PCR reaction) and after 40 cycles (saturated PCR) and further processed according to MRTU detection protocol. Relative RTU activities values were calculated as described in **Figure 2b**. Error bars, mean ±s.d. of the three independent PCRs.

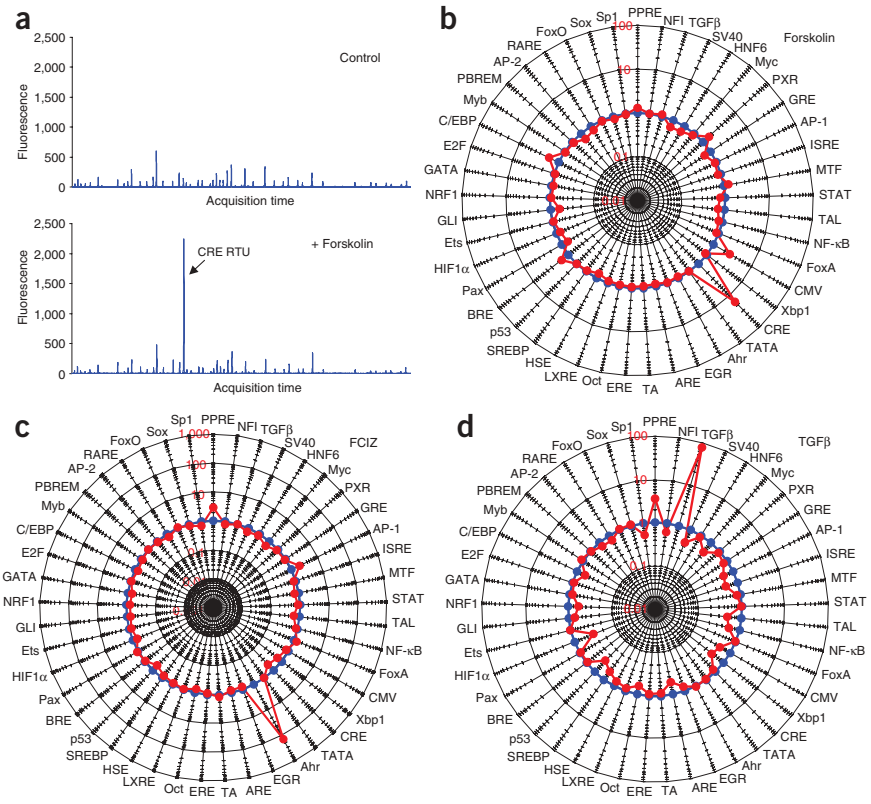

Figure 4 | Evaluation of biologically active compounds using MRTU assay. (**a**) Representative capillary electrophoresis readouts of MRTU assay in the untreated (Control) HepG2 cells and in the cells treated with 25 μM forskolin for 4 h. (**b**–**d**) Forskolin- (25 μM; **b**), FCIZ- (1 μM; **c**) or TGFβ- (final concentration of 1 ng/ml; **d**) induced TF activity profiles calculated by dividing specific (TATA RTU–normalized) TF activity profiles in the treated cells by those in the untreated cells. For each compound, the data represent mean of fold-induction values of individual RTUs obtained in three independent experiments performed in parallel. Note that data are plotted in a log scale, and that the fold-induction values in the untreated cells, by definition, are equal to 1.0.

high-quality multiplexing gene expression platforms[14]. We assessed linearity of the assay by comparing the signals produced by titrated calibrating SV40 RTUs. Linearity was nearly perfect ($R^2 = 0.9992$), indicating that the RTU activity profiles were not distorted despite the exponential nature of PCR amplification (**Fig. 2b**).

Because transfection efficiency can vary broadly between experiments and among different cell types, we assessed consistency of the results obtained in experiments when different amounts of the MRTU library were used. We found that titration of the reporter DNA library from 500 ng to 20 ng per transfection caused no apparent effects on the TF activity profile (**Fig. 3a**).

We also evaluated the sensitivity of the assay to variations in integrity of the isolated RNA. We assayed RNA samples with substantially different amounts of RNA degradation and found no differences between the assay readouts (**Fig. 3b**).

Finally, to evaluate the potential variability resulting from differences in PCR amplification, we assessed the TF activity profiles after altering the number of PCR amplification cycles. We found that MRTU assay results were identical when we used PCR products collected during either exponential or saturation phases of the reaction (**Fig. 3c**).

We believe that the robustness of the MRTU assay stems from the similarity of the individual reporter transcripts,

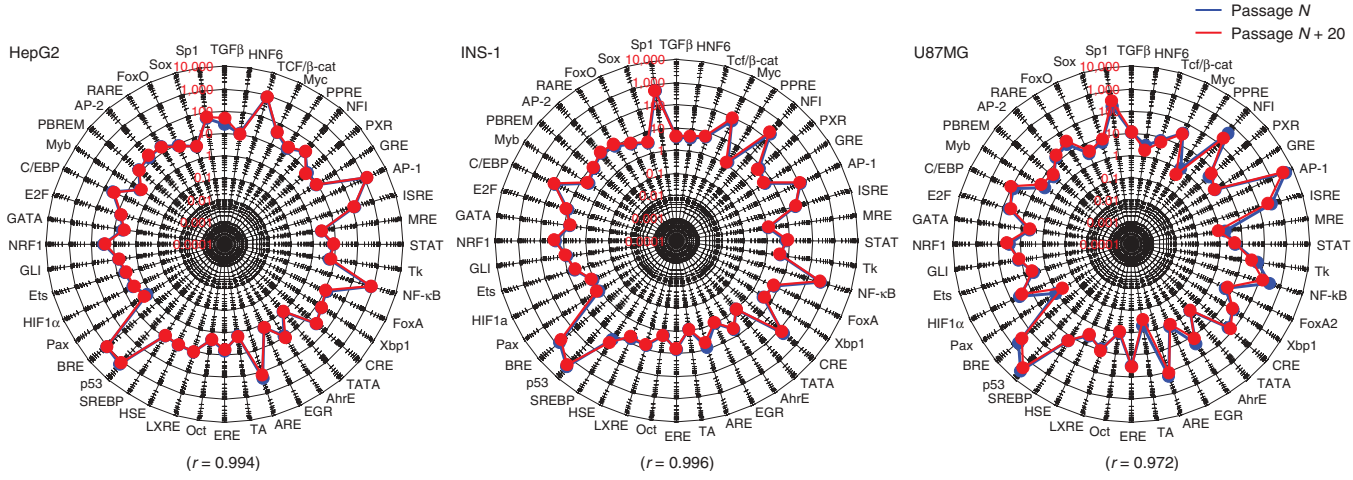

Figure 5 | Profile of TF activities provides a distinct cell signature that is stable over time. Human, HepG2 and U87MG, and rat, INS-1, cell lines were maintained for 20 consecutive passages in culture under identical growth conditions. Cells underwent an estimated five population doublings at each passage. Basal TF activity profiles were determined at passages *N* and *N* + 20 by transiently transfecting the cells with prototypical MRTU library and by using the MRTU detection protocol, as described in **Figure 2**. Each TF activity profile represents mean values of three independent experiments performed in parallel. Pair-wise correlations (*r*) between the profiles were calculated by using Pearson's metric.

which are equally affected by the variations in test conditions, and thus their relative concentrations remain unchanged.

TF signatures of biologically active molecules

We next accessed the feasibility of using our MRTU assay to characterize biological properties of various stimuli and compounds by exposing cells to these agents and analyzing the induced alterations in the TF activity profile. We transiently introduced the MRTU library into HepG2 cells and assessed TF activity profiles before and after stimulation with various prototypical inducers, including 6-formylindolo carbazole (FICZ), a high affinity agonist of the aryl hydrocarbon receptor (AhR) pathway[15]; forskolin, an activator of adenylate cyclase and prototypical inducer of cAMP-dependent pathway[16]; and TGFβ, a prototypical inducer of TGFβ pathway[17]. The major changes elicited in the TF activity profile were consistent with the known specific properties of the stimuli. That is, FICZ, forskolin and TGFβ potently activated AhrE RTU (139-fold induction, $P = 0.00014$), CRE RTU (a 16-fold induction, $P = 0.00007$) and TGFβ RTU (78-fold induction, $P = 0.0005$), respectively (**Fig. 4**). There were also other, subtler, yet statistically significant, responses. For example, forskolin activated the C/EBP RTU (1.75-fold induction, $P = 0.002$); TGFβ activated the PPRE RTU (3.6-fold induction, $P = 0.0023$) but inhibited c-Myc RTU (0.54-fold induction, $P = 0.0009$), p53 RTU (0.44-fold induction, $P = 0.0013$), HIF1α RTU (0.34-fold induction, $P = 0.01$) and Xbp1 RTU (0.46-fold induction, $P = 0.01$), whereas FICZ activated the PPRE RTU (a 2.8-fold induction, $P = 0.0005$) (**Fig. 4** and **Supplementary Table 4** online). Notably, we reproduced these responses in independent experiments performed at different times and in different batches of HepG2 cells (**Supplementary Fig. 4** online).

TF activity profile represents distinct cellular signatures

To use TF activity profile as potential cell signature, we determined how different distinct TF activity profiles were in different cell types as compared to temporal fluctuations of these profiles. To quantitatively compare TF activity profiles, we used an approach similar to that used for comparing gene expression profiles in transcriptomics[18]. Accordingly, we considered a TF activity profile as an N-dimensional vector whose coordinates are determined by the specific activity values of the N RTUs. In this approach, the similarity of any two TF activity profiles is a function of distance between these vectors, which can be evaluated by different means, for example, as the Pearson's correlation[18]. Using this metric, we quantitatively compared the temporal and cell type–specific differences of TF activity profiles in several established human and rat cell lines. We found that for each particular cell type we tested, the TF activity profile was a remarkably reproducible characteristic that did not change over many cell generations (**Fig. 5**). The dissimilarities between TF activity profiles obtained from different passages of each cell type were negligibly small as compared to the differences of TF profiles of distinct cell

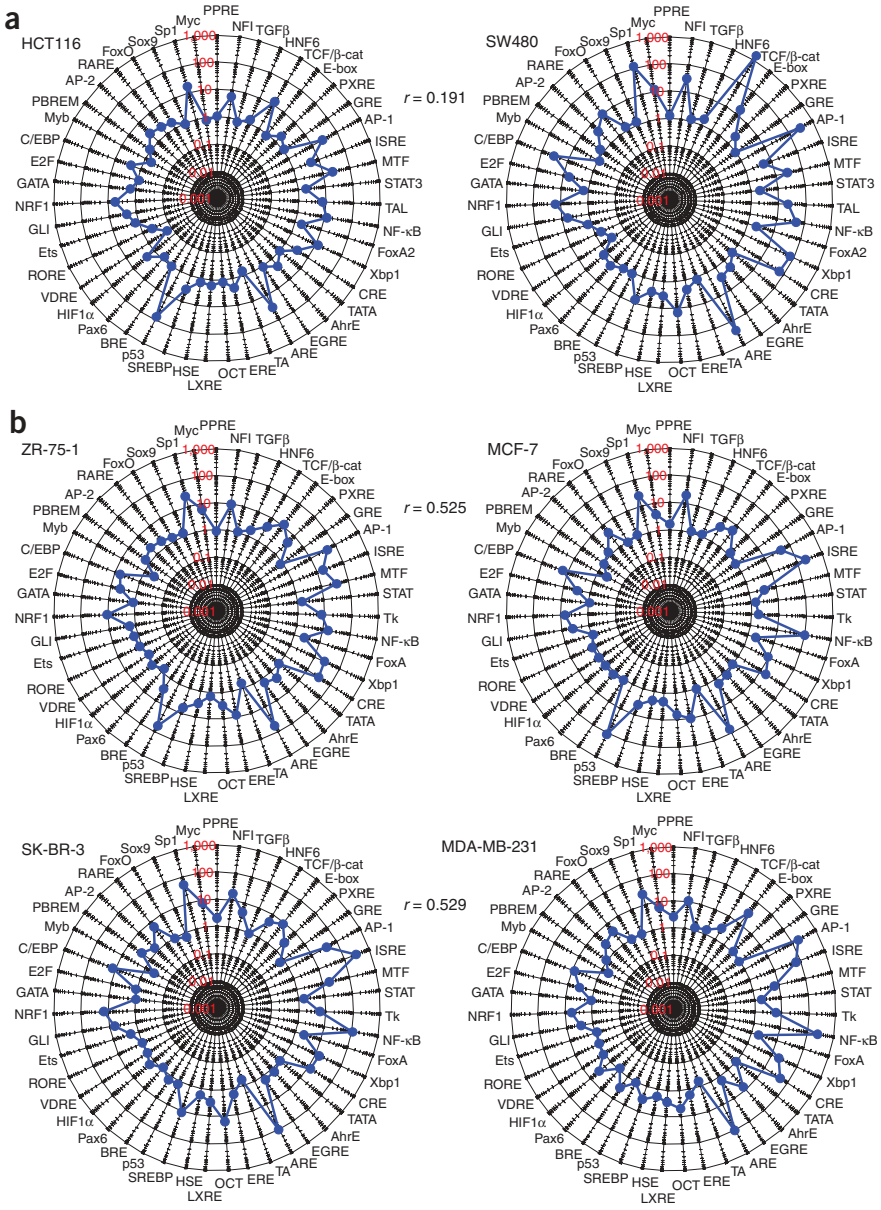

Figure 6 | Anatomically related cancer cells have distinct TF activity profiles. (**a**,**b**) Human colorectal cancer cell lines SW480 and HCT116 (**a**), and human breast cancer cell lines ZR-75-1, MCF-7, MDA-MB-231 and SK-BR-3 (**b**) were maintained under identical growth conditions. The basal TF activity profiles were obtained by transiently transfecting the cells with prototypical MRTU library and by following the MRTU detection protocol. Data were calculated as described in **Figure 2.** Each graph represents profile of mean values of specific RTU activities obtained in three independent experiments performed in parallel. Pair-wise correlations (r) between the profiles were calculated using Pearson's metric.

types. In fact, TF activity profiles at passages N and $N + 20$ were so similar that the corresponding graphs almost completely overlapped (**Fig. 5**). Thus, we concluded that TF activity profile represents a robust signature of cell.

Analyzing cancer-related alterations of TF activity profiles

We compared TF activity profiles in several cancer cell lines of closely related anatomic origins: two human colorectal carcinomas and four human breast carcinomas. It is well established that the pattern of gene expression for different cancer cell lines of the related histological origins largely overlap[19–22]. In contrast, TF activity profiles were clearly distinct even in closely related cancer cell types (**Fig. 6** and **Supplementary Table 5** online). For example, we found a low similarity between TF activity profiles of two luminal breast carcinomas ZR-75-1 and MCF-7 ($r = 0.525$) and of two colorectal carcinomas SW480 and HCT116 ($r = 0.191$), whereas cells of different origins (breast carcinoma ZR-75-1 and colorectal carcinoma HCT116) showed a much higher similarity ($r = 0.833$), suggesting that TF activity profiles could relate cancer cells not according to their tissue origin, but rather by commonality of underlying mechanisms of their transformation.

We found many features of the TF activity profiles that were in agreement with previously published data. For example, a high activity of TCF/β-catenin RTU in SW480 colorectal carcinoma cells was consistent with published data[23,24]; a high NF-κB RTU activity in MDA-MB-231 breast carcinoma cells is consistent with reported constitutively active NF-κB in these cells[25]. Furthermore, the activity of p53 RTU correlated with the functional status of tumor-suppressor p53 protein, that is, cells with wild-type p53 (ZR-75-1, MCF-7 and HCT116[26,27]) showed a high p53 RTU activity, in contrast to cells that had mutant p53 (SW480, MDA-MB-231 and SK-BR-3 cells[28–30]). Akin to that, estrogen receptor–positive ZR-75-1 and MCF-7 cells[31] showed a high ERE RTU activity as compared to estrogen receptor–negative (MDA-MB-231 and SK-BR-3 cells[31]) (**Fig. 6**). These data demonstrate that TF profiling technology can be used to reveal disease-related alterations occurring in signal transduction networks in cancer cells.

DISCUSSION

The prototypical MRTU library described here afforded evaluation of 43 distinct *cis*-regulatory RTUs. The assessment content can be readily scaled up by including additional RTU plasmids in the library. Hundreds of *Hpa*I-tagged reporter sequences are available for this purpose, and the single-base resolution of capillary electrophoresis instruments is sufficient to analyze hundreds of additional RTU peaks. Thus, we believe that we could gradually develop an MRTU platform to analyze activities of several hundred of already annotated mammalian TFs[3] and, ultimately, the entire complement of mammalian TFs.

In its current form, our prototypical MRTU assay has certain technical limitations. First, the assay depends on efficient transfection. We successfully used the plasmid-based MRTU library to analyze dozens of various cell types, including established human and mouse cell lines and primary cell cultures, such as mouse and rat hepatocytes, embryo fibroblasts and human skin fibroblasts (data not shown). However, some cell types are refractory to transfection. To obviate this limitation, RTUs may be cloned into the backbone of appropriate delivery vehicle, for example, a recombinant viral vector. Another limitation is that the standard capillary electrophoresis fluorescence detectors that are used in DNA sequencers have a rather narrow (about 100-fold) linear detection range. This limits the accuracy of detection for very strong and very weak signals. This limitation can be obviated either by using fluorescent detectors with a larger dynamic range, or by analyzing several dilutions of the sample.

Despite the limitations, the remarkable robustness and accuracy exhibited by our technology allowed us for the first time to perform truly quantitative assessments of TF activity profiles in different cell types and under different conditions. We established that TF activity profiles represent robust and sustained signatures that do not change over many cell generations and that are quite distinct for different cell types. These data justified the use of TF activity profiling for high-content analyses of cellular regulation.

The TF-profiling technology that we developed should find many biomedical applications. Here we demonstrated a few of them, By introducing the MRTU library into cells we produced a new type of cell-based biosensors that characterize evaluated stimuli according to the elicited alterations in TF activity profiles. This approach is not dissimilar from other toxicogenomic approaches, when compounds are characterized by elicited changes in gene expression profiles[32]. However, the TF-profiling technology has a distinct advantage in that it affords direct identification of the involved pathways and thus allows clear-cut interpretation.

Another potential application of the TF profiling technology that we described here deals with analyzing mechanisms underlying cancer cell pathology. We showed that cancer cell lines, even those derived from anatomically related cancer lesions, can be distinguished according to their TF activity profiles. This observation suggests a new approach to identification of cancer-related abnormalities of signal transduction pathways, and to development of personalized approaches to cancer treatment.

There are many other potential applications, including gene-function annotation in the context of signal transduction, evaluation of drug candidates and toxic substances. In this regard, we expect that the TF profiling technology will greatly synergize with other system biology approaches, such as transcriptomics and proteomics.

METHODS

MRTU detection protocol. We routinely transfected cells with the MRTU library in a six-well plate format by using FuGene 6 reagent (Roche; 3 μl FuGene/1 μg DNA). We isolated total RNA using TriZol reagent (Invitrogen), treated it with DNAse I (Ambion) for 30 min, and reverse transcribed the RNA using oligo(dT) primer and Mo-MLV reverse transcriptase (Invitrogen). By PCR, we amplified one-tenth of the reverse-transcribed RNA using *Taq* DNA polymerase (Invitrogen) and two reporter sequence–specific primers (**Supplementary Fig. 1**). We labeled the PCR products by primer extension with 6-carboxyfluorescein (6-FAM) 5′-labeled reporter sequence–specific primer (2 min at 95 °C, 20 s at 68 °C and 10 min at 72 °C) and then digested the products with 5U of *Hpa*I (New England Biolabs) for 2 h at 37 °C. Using Qiaquick PCR columns (Qiagen) we purified the fragments and analyzed them on an ABI 3130xL genetic analyzer (Applied Biosystems). Peaks' positions were identified by using a set of X-rhodamine (ROX)-labeled MapMarker1000 molecular weight standards (BioVentures).

MRTU assay data analysis. We processed raw capillary electrophoresis data using Attagraph software (Attagene). We determined

Pearson product-moment correlation of TF activity profiles as

$$Cor_{(A,B)} \equiv \frac{\sum_n (A_n - \langle A \rangle) \times (B_n - \langle B \rangle)}{\sqrt{\sum_n (A_n - \langle A \rangle) \times (A_n - \langle A \rangle)} \times \sqrt{\sum_n (B_n - \langle B \rangle) \times (B_n - \langle B \rangle)}},$$

where A and B represent two different TF profiles, each comprising specific activity values of N individual TFs: $(A_1, A_2, A_3 \ldots A_N)$ and $(B_1, B_2, B_3 \ldots B_N)$, respectively, and $\langle A \rangle$ and $\langle B \rangle$ represent the mean of values of all individual TFs activities of profiles A and B.

We evaluated the statistical significance of the observed changes by two-tailed Student's *t*-test using data obtained from at least three independent experiments performed in parallel.

Additional methods. Cell culture conditions and details on construction of individual RTUs are available in **Supplementary Methods** online.

Note: Supplementary information is available on the Nature Methods website.

ACKNOWLEDGMENTS

We thank S. Langdon for invaluable help with fragment analysis, and A.S. Baldwin and R. Gaynor for discussions. The work was supported by US National Institutes of Health grants 1R43CA101636, 1R43CA101271 and U01 AI061360.

AUTHOR CONTRIBUTIONS

S.R., A.M. and S.M. are authors of the concept. A.M. and M.M. constructed the RTU library; A.M. and S.R. designed the experiments; Ma.G., M.M., N.P., L.M. and L.D. performed the experiments; Mi.G. designed the software; S.R. and S.M. wrote the manuscript.

COMPETING INTERESTS STATEMENT

The authors declare competing financial interests: details accompany the full-text HTML version of the paper at http://www.nature.com/naturemethods/.

Published online at http://www.nature.com/naturemethods/
Reprints and permissions information is available online at http://npg.nature.com/reprintsandpermissions

1. Babu, M.M., Luscombe, N.M., Aravind, L., Gerstein, M. & Teichmann, S.A. Structure and evolution of transcriptional regulatory networks. *Curr. Opin. Struct. Biol.* **14**, 283–291 (2004).
2. Stegmaier, P., Kel, A.E. & Wingender, E. Systematic DNA-binding domain classification of transcription factors. *Genome Inform.* **15**, 276–286 (2004).
3. Matys, V. *et al.* TRANSFAC and its module TRANSCompel: transcriptional gene regulation in eukaryotes. *Nucleic Acids Res.* **34** Database issue, D108–D110 (2006).
4. Benotmane, A.M., Hoylaerts, M.F., Collen, D. & Belayew, A. Nonisotopic quantitative analysis of protein-DNA interactions at equilibrium. *Anal. Biochem.* **250**, 181–185 (1997).
5. Rosenau, C., Emery, D., Kaboord, B. & Qoronfleh, M.W. Development of a high-throughput plate-based chemiluminescent transcription factor assay. *J. Biomol. Screen.* **9**, 334–342 (2004).
6. Hermanson, O., Glass, C.K. & Rosenfeld, M.G. Nuclear receptor coregulators: multiple modes of modification. *Trends Endocrinol. Metab.* **13**, 55–60 (2002).
7. Bronstein, I., Fortin, J., Stanley, P.E., Stewart, G.S. & Kricka, L.J. Chemiluminescent and bioluminescent reporter gene assays. *Anal. Biochem.* **219**, 169–181 (1994).
8. Kovacs, D.M. & Kaplan, B.B. Discordant estimates of heterologous promoter activity as determined by reporter gene mRNA levels and enzyme activity. *Biochem. Biophys. Res. Commun.* **189**, 912–918 (1992).
9. Li, X., Jiang, X. & Yaoi, T. High throughput assays for analyzing transcription factors. *Assay Drug Dev. Technol.* **4**, 333–341 (2006).
10. Guhaniyogi, J. & Brewer, G. Regulation of mRNA stability in mammalian cells. *Gene* **265**, 11–23 (2001).
11. Shim, J. & Karin, M. The control of mRNA stability in response to extracellular stimuli. *Mol. Cells* **14**, 323–331 (2002).
12. Levitt, N., Briggs, D., Gil, A. & Proudfoot, N.J. Definition of an efficient synthetic poly(A) site. *Genes Dev.* **3**, 1019–1025 (1989).
13. Enriquez-Harris, P., Levitt, N., Briggs, D. & Proudfoot, N.J. A pause site for RNA polymerase II is associated with termination of transcription. *EMBO J.* **10**, 1833–1842 (1991).
14. MAQC Consortium. The MicroArray Quality Control (MAQC) project shows inter- and intraplatform reproducibility of gene expression measurements. *Nat. Biotechnol.* **24**, 1151–1161 (2006).
15. Oberg, M., Bergander, L., Hakansson, H., Rannug, U. & Rannug A. Identification of the tryptophan photoproduct 6-formylindolo[3,2-b]carbazole, in cell culture medium, as a factor that controls the background aryl hydrocarbon receptor activity. *Toxicol. Sci.* **85**, 935–943 (2005).
16. Montminy, M.R. & Bilezikjian, L.M. Binding of a nuclear protein to the cyclic-AMP response element of the somatostatin gene. *Nature* **328**, 175–178 (1987).
17. Dennler, S. *et al.* Direct binding of Smad3 and Smad4 to critical TGF beta-inducible elements in the promoter of human plasminogen activator inhibitor-type 1 gene. *EMBO J.* **17**, 3091–3100 (1998).
18. Eisen, M.B., Spellman, P.T., Brown, P.O. & Botstein, D. Cluster analysis and display of genome-wide expression patterns. *Proc. Natl. Acad. Sci. USA* **95**, 14863–14868 (1998).
19. Zhang, L. *et al.* Gene expression profiles in normal and cancer cells. *Science* **276**, 1268–1272 (1997).
20. Perou, C.M. *et al.* Molecular portraits of human breast tumours. *Nature* **406**, 747–752 (2000).
21. Okabe, H. *et al.* Genome-wide analysis of gene expression in human hepatocellular carcinomas using cDNA microarray: identification of genes involved in viral carcinogenesis and tumor progression. *Cancer Res.* **61**, 2129–2137 (2001).
22. Ross, D.T. *et al.* Systematic variation in gene expression patterns in human cancer cell lines. *Nat. Genet.* **24**, 227–235 (2000).
23. Korinek, V. *et al.* Constitutive transcriptional activation by a beta-catenin-Tcf complex in APC−/− colon carcinoma. *Science* **275**, 1784–1787 (1997).
24. Morin, P.J. *et al.* Activation of beta-catenin-Tcf signaling in colon cancer by mutations in beta-catenin or APC. *Science* **275**, 1787–1790 (1997).
25. Nakshatri, H., Bhat-Nakshatri, P., Martin, D.A., Goulet, R.J. Jr. & Sledge, G.W. Jr. Constitutive activation of NF-kappaB during progression of breast cancer to hormone-independent growth. *Mol. Cell. Biol.* **17**, 3629–3639 (1997).
26. Troester, M.A. *et al.* Cell-type-specific responses to chemotherapeutics in breast cancer. *Cancer Res.* **64**, 4218–4226 (2004).
27. Waldman, T., Lengauer, C., Kinzler, K.W. & Vogelstein, B. Uncoupling of S phase and mitosis induced by anticancer agents in cells lacking p21. *Nature* **381**, 713–716 (1996).
28. Goyette, M.C. *et al.* Progression of colorectal cancer is associated with multiple tumor suppressor gene defects but inhibition of tumorigenicity is accomplished by correction of any single defect via chromosome transfer. *Mol. Cell. Biol.* **12**, 1387–1395 (1992).
29. Shao, Z.M. *et al.* p53 independent G0/G1 arrest and apoptosis induced by a novel retinoid in human breast cancer cells. *Oncogene* **11**, 493–504 (1995).
30. Sugikawa, E. *et al.* Mutant p53 mediated induction of cell cycle arrest and apoptosis at G1 phase by 9-hydroxyellipticine. *Anticancer Res.* **19**, 3099–3108 (1999).
31. Tamaru, N. *et al.* Estrogen receptor-associated expression of keratinocyte growth factor and its possible role in the inhibition of apoptosis in human breast cancer. *Lab. Invest.* **84**, 1460–1471 (2004).
32. Nuwaysir, E.F., Bittner, M., Trent, J., Barrett, J.C. & Afshari, C.A. Microarrays and toxicology: the advent of toxicogenomics. *Mol. Carcinog.* **24**, 153–159 (1999).